BIOPOLYMERS VOL. 15, 1655–1667 (1976)

Circular Dichroism and Structure of the Complex of Acridine Orange with Poly(L-glutamic Acid)

TOYOKO IMAE and SHOICHI IKEDA, *Department of Chemistry, Faculty of Science, Nagoya University, Nagoya, Japan*

Synopsis

Circular dichroism and absorption spectra have been measured on solutions of acridine orange and poly(L-glutamic acid) mixed at two molar ratios of carboxyl group-to-dye, P/D 25 and 0.8, and at different pH's. Characteristic circular dichroism is induced at the absorption bands of acridine orange when the P/D is 25 and the solution is acidic. Another type of circular dichroism is manifest at neutral and alkaline pH when P/D is 0.8. For the induction of the former type of circular dichroism, a helical array of acridine-orange dimers bound to the α-helix is postulated, in which the dye molecular planes are almost perpendicular to the helical axis. Assuming the helical geometry and optical parameters, combined with the observed magnitude of transition electric moment, the rotatory strength of the complex is calculated to the zeroth order approximation, and the observed circular dichroism spectra have been reproduced.

INTRODUCTION

The extrinsic Cotton effect induced on aqueous solutions of cationic dyes added to α-helical poly(L-glutamic acid) was first discovered by Blout and Stryer.[1] Since then, the optical activity induced on acridine orange in the presence of poly(L-glutamic acid) has been investigated by many workers.[2–6] It was observed in acid solutions, where the α-helical conformation of poly(L-glutamic acid) is stable, and with mixtures of relatively high residue-to-dye molar ratios, P/D. Stryer and Blout[2] suggested three possible models for the complex formed between dye and α-helical polypeptide. In the case of acridine orange, they claimed two kinds of helical arrangement of dye molecules, attributable to the origin of each of two Cotton effects observed in the visible region. Ballard et al.[3] proposed a more definitive model for the complex, based on the observations of flow circular dichroism and an erroneous modification[7] of the Moffitt theory of optical activity.[8,9] In their model, dye molecules form a left-handed helix around an α-helical polypeptide, the longer axis of dye molecular plane being close to parallel to the helical axis.

On the other hand, when the mixing ratio, P/D, is about 1, different kinds of Cotton effects were observed with aqueous solutions of acridine orange mixed with poly(L-glutamic acid) at neutral or alkaline pH, where poly(L-glutamic acid) is in a randomly coiled conformation.[5,6,10–13]

In the present paper we will summarize various types of optical activity

induced on acridine orange when mixed with poly(L-glutamic acid), either helical or random coil. Furthermore, we propose a possible model for the complex of acridine orange formed with α-helical poly(L-glutamic acid) and calculate the optical rotatory power by means of the zeroth order perturbation theory.

EXPERIMENTAL

Materials

Sodium poly(L-glutamate monohydrate) (#G-32) was obtained from the Pilot Chemical Co., Ltd. Acridine orange was purified from the commercial zinc chloride salt, as previously described,[14,15] and obtained as the hydrochloride salt.

Preparation of Solutions

To an aqueous solution of sodium poly(L-glutamate), a stock solution of acridine orange was added to give a desired P/D ratio, usually 25 or 0.8; the pH was adjusted by HCl or NaOH solution. The final dye concentration was made to 4.94×10^{-5} M in most cases. The spectra were measured on the solutions kept overnight after its preparation.

Measurements

The pH of the solutions was measured with a Hitachi–Horiba F5-X pH-meter. Absorption spectra were recorded on a Hitachi 323 Recording Spectrophotometer over the wavelength region from 600 to 350 nm, using a 5-mm quartz cell. Circular dichroism measurements were carried out on a Jasco J-20 Circular Dichrometer from 620 to 185 nm, using either a 10 or 1 mm cell. The latter cell was used for the determination of circular dichroism of the solutions of P/D 25 at the far ultraviolet region. The circular dichrometer was calibrated with an aqueous solution of d-10-camphor sulfonic acid.[16] All the measurements were performed at room temperature (ca. 25°C). The molar extinction coefficient, ϵ_D, and molar ellipticity, $[\theta_D]$, were calculated based on the total concentration of added dye.

RESULTS

Solutions of P/D 25 (Acridine Orange-α-Helix Systems)

The visible absorption spectra of acridine orange in water are characterized by two bands at 492 and 470 nm, when the dye concentration is about 5×10^{-5} M.[14,15] When poly(L-glutamic acid) is added to P/D 25, the main absorption band shifts to blue around 450–457 nm, and a weak shoulder appears at 510 nm. This is shown in Figure 1. The blue shift and

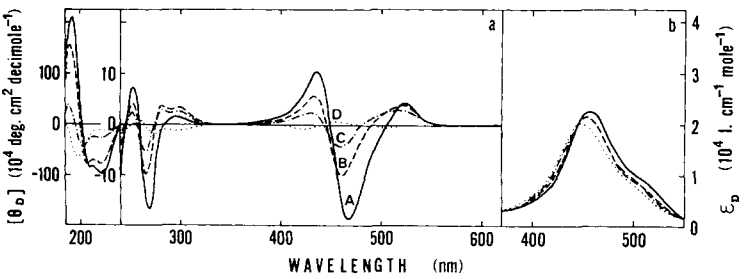

Fig. 1. Circular dichroism (a) and absorption spectra (b) of the acridine orange-poly(L-glutamic acid) system of P/D 25 in water. $[D] = 4.94 \times 10^{-5} M$. Curve A: pH 4.05. Curve B: pH 5.87. Curve C: pH 6.28. Curve D: pH 6.71.

hypochromism suggest the formation of highly aggregated dimeric dye and nearly total binding of added dye to the polymer.[15,17] While the absorption spectra are not very dependent on the pH when it is lower than 10, the circular dichroism reflects the occurrence of pH-induced helix–coil transition of the polypeptide moiety.

In acidic pH, as Figure 1 shows, the circular dichroism spectra at the far-ultraviolet region consist of a strongly positive band at 191 nm and two negative bands at 210 and 222 nm, and clearly indicate the presence of α-helix.[9,16] Circular dichroism is induced at the absorption region of acridine orange. A strongly negative circular dichroic band is observed at 466 nm and two positive bands are at 523 and 436 nm. Similarly, in the ultraviolet region, where acridine orange absorbs at 261 and 290 nm, a strongly negative band is at 268 nm and two positive bands are at 295 and 253 nm. The circular dichroism is similar to that previously observed.[3–5,11] It was designated as Type IV circular dichroism.[17]

With increasing pH, the far-ultraviolet circular dichroism decreases its magnitude, and the helical conformation of poly(L-glutamic acid) is destroyed, indicating the occurrence of pH-induced helix-to-coil transition.[18] The induced circular dichroism also generally decreases its magnitude. Up to pH 6.5, however, the positive band at 523 nm retains its magnitude, while the positive band at 295 nm increases with increasing pH. Further increase in the pH reduces their magnitudes, and no circular dichroism is observed at neutral or alkaline pH.

Solutions of P/D 0.8 (Acridine Orange-Random Coil Systems)

While the solution of P/D 25 separates red precipitates at a pH lower than 3.4, the solution of P/D 0.8 forms red gel at the pH region over 3.2 to 6.3. Figure 2 shows the absorption and circular dichroism spectra of solutions of P/D 0.8 at various pH, where the solutions are homogeneous. The main absorption band is always located at 492 nm and a strong shoulder is at 470 nm. Thus the monomeric form of the dye is predominantly present. The hypochromic effect is very strong at a pH higher than 6.3 and is stronger as the pH is raised, indicating the strong binding of dye to the polymer.

TABLE I
Circular Dichroism of Acridine Orange-Poly(L-glutamic Acid)

P/D	25	1[a]	0.8
Visible CD bands[b] (nm)	523(+)m 466(−)s 436(+)m	540(+)sh 470(+)s 420(−)m	557(+)s 421(−)m
Unit of bound dye	Dimer		Monomer
Polymer conformation	α-helix		(Random coil)
pH	4.1–6.3	6–12	6.8–10.5
Type of CD	IV		III′

[a] Reference 12.
[b] s:strong; m:medium; sh:shoulder.

The visible circular dichroism observed in the same pH region is characterized by a strong positive band at 557 nm, a positive shoulder at 500 nm, and a negative band at 421 nm. The ultraviolet band has a positive circular dichroism band at 340 nm, and negative bands at 280, 250, and 220 nm. This type of circular dichroism was designated as Type III′ circular dichroism in a previous paper.[17] Some workers[11,12] reported that the induced circular dichroism of the solution of P/D 1 at alkaline pH has a strong positive band at 470 nm and a weaker positive shoulder at 540 nm, followed by a negative band at 420 nm. This circular dichroism is certainly due to the dimeric dye molecules bound to the polymer. It belongs to the Type III circular dichroism.[17] Since poly(L-glutamic acid) is randomly coiled and highly charged in this pH region, all the carboxylate groups on the side chains would be occupied by the cationic dye molecules. Table I summarizes different types of circular dichroism observed for acridine orange-poly(L-glutamic acid) systems.

At a pH lower than 3.2, where the mixture is again homogeneous, the absorption spectra are scarcely distinguishable from those of free dye solutions. This indicates that only a few of the dye molecules are bound to the polymer, possibly owing to the very low ionization of carboxyl groups. Thus, the apparent induced circular dichroism is weak, as seen in Figure 2. It reduces further with lowering pH and becomes zero at a pH lower than 2.26.

DISCUSSION

Helical Arrangement of Acridine Orange Bound to the α-Helix

In this paper we will discuss the mechanism of induction of circular dichroism of acridine orange in the presence of α-helical poly(L-glutamic acid), which is illustrated in Figure 1.

Since the binding of acridine orange with poly(L-glutamic acid) is primarily electrostatic, the binding of acridine orange with α-helical poly(L-glutamic acid) must occur in a helical array, if any regularity and dissymmetry are required for the extrinsic optical activity to be induced. This

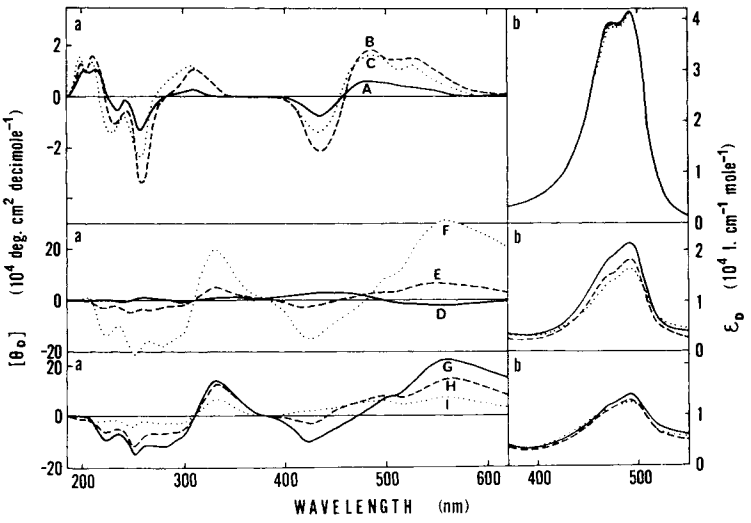

Fig. 2. Circular dichroism (a) and absorption spectra (b) of the acridine orange-poly(L-glutamic acid) system of P/D 0.8 in water. $[D] = 4.94 \times 10^{-5} M$. Curve A: pH 2.68. Curve B: pH 2.90. Curve C: pH 3.06. Curve D: pH 6.51. Curve E: pH 6.81. Curve F: pH 7.00. Curve G: pH 7.32. Curve H: pH 7.55. Curve I: pH 9.01.

is the Model II of Stryer and Blout.[2] We assume that bound dye is in dimeric molecules of antiparallel type, such as proposed by Zanker[14], since the visible absorption band is located at the blue-shifted wavelength. If more than four dimeric dye molecules were attached consecutively on carboxyl groups along the polypeptide chain, steric hindrance would always occur among the dye molecules. Instead, we propose the following model for the dye-α-helix complex.

The helical array of dimeric dye molecules is formed along the polypeptide backbone, in which each molecule occupies two contiguous carboxyl groups and thus its molecular plane is parallel to the smoothed backbone helix. Figure 3 illustrates the structure of the complex. The number of dimeric dye molecules per helical turn, P, must be half that of the amino-acid residues in the α-helix, i.e., $P = 1.8$. The pitch of the superhelix per bound dimeric dye molecule, b, is then twice, i.e., $b = 3.0$ Å. The radius of the superhelix, i.e., the distance of the chromophore center from the helix axis, a, was taken to be 6.0 Å. Since the distance between two consecutive carboxyl groups is about 9.3 Å and the nitrogen atoms of dimethylamino groups are about 9.8 Å apart, the dye molecule can bind with the consecutive carboxyl groups through these nitrogen atoms. In this connection, it is noted that the distance between the third neighbor carboxyl groups is about 7.5 Å and the distance between the fourth neighbors is about 7.3 Å. The longer axis of molecular plane is put perpendicular to the radial direction ($\phi = 90°$) and tilted against the helix axis by 80° ($\theta = 80°$), so that it is nearly parallel to the smoothed polypeptide helix. These values of geometric parameters for the dye helix are summarized in Table II.

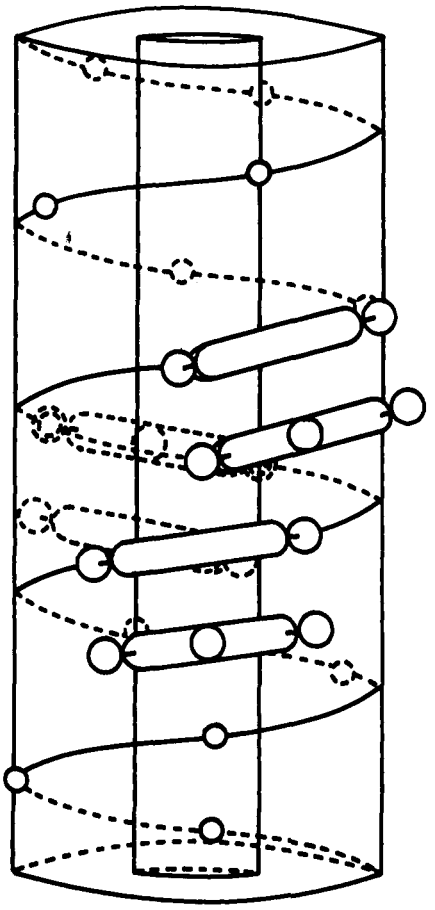

Fig. 3. Model proposed for the acridine orange-α-helix polymer complex.

Calculation of Circular Dichroism

Generally, an electronic excited state of chromophore splits into N levels when N identical chromophores are arranged in a helical way. With the transition between the ground state and each exciton level of the excited

TABLE II
Geometric Parameters for Assumed Helices of the Complex

Dye Molecules Anchor On	a (Å)	b (Å)	P (Chromophores/Turn)	θ[a] (deg)	ϕ (deg)
1-2	6.0	3.0	1.8	80	90
1-4	6.0	1.5	3.6	125	90
1-5	6.0	1.5	3.6	35	90
1-4-7	6.0	10.5	1.06	125	90

[a] $\theta > 90$ means $\mu_{oe,t}\mu_{oe,\parallel} < 0$.

state of the array are associated a dipole strength and a rotatory strength which can be calculated by the method of Tinoco et al.[19] If the electric dipole moment of a chromophore for the transition, $0 - e$, has the components parallel and perpendicular to the helix axis, $\mu_{0e,\parallel}$ and $\mu_{0e,\perp}$, respectively, and a tangential component along the helix-advancing direction, $\mu_{0e,t}$, then the dipole strength, D_{EK}, and the rotatory strength, R_{EK}, associated with the Kth level of an excited state, E, of the right-handed helical array are given by

$$D_{EK} = \mu_{0e,\parallel}^2 \left\{1 + \sum_{k=1}^{N} \sum_{l \neq k}^{N}{}' C_{keK} C_{leK}\right\} + \mu_{0e,\perp}^2 \left\{1 + \sum_{k=1}^{N} \sum_{l \neq k}^{N}{}' C_{keK} C_{leK} \cos \frac{2\pi}{P}(l-k)\right\} \quad (1)$$

and

$$R_{EK} = \frac{\pi \nu_{E0}}{c} a \mu_{0e,\parallel} \mu_{0e,t} \sum_{k=1}^{N} \sum_{l \neq k}^{N}{}' C_{keK} C_{leK} \left\{1 - \cos \frac{2\pi}{P}(l-k)\right\} - \frac{\pi \nu_{E0}}{2c} b \mu_{0e,\perp}^2 \sum_{k=1}^{N} \sum_{l \neq k}^{N}{}' C_{keK} C_{leK} (l-k) \sin \frac{2\pi}{P}(l-k) \quad (2)$$

respectively, and the frequency is written as

$$\nu_{EK} = \nu_{E0} + E'_{EK}/h \quad (3)$$

where c is the light velocity, h is the Planck constant, and ν_{E0} stands for the unperturbed frequency of chromophore. The perturbation, E'_{EK}, and the exciton coefficient, C_{keK}, can be obtained by solving a set of linear equations

$$\sum_{k=1}^{N} C_{keK}(V_{k0e,l0e} - \delta_{k,l} E'_{EK}) = 0, \qquad l = 1, 2, \cdots, N \quad (4)$$

and orthonormal conditions

$$\sum_{K=1}^{N} C_{keK} C_{leK} = \delta_{k,l} \quad (5)$$

where $V_{k0e,l0e}$ is the dipole–dipole interaction potential between kth and lth chromophores and $\delta_{k,l}$ is the Kronecker's delta.

We are concerned with circular dichroism associated with the two transitions, 458 ($e = a$) and 261 ($e = b$) nm, both of which are due to the dimeric dye molecule and have transition electric moments parallel to the longer axis of the dye molecular plane.[15,20,21] The magnitude of the electric dipole moment for the visible transition, $0 - a$, was estimated from the observed absorption spectra by means of

$$\mu_{0a}^2 = 2(6909/8\pi^3 N_A) \int_A (\epsilon_D/\nu) d\nu \quad (6)$$

where ν is the frequency and N_A is the Avogadro number. The factor 2 was introduced for conversion from the monomer to dimer basis of the dye. The observed spectra are nearly independent of pH at the alkaline region. A weak shoulder at 510 nm possibly corresponds to the parallel component of exciton splitting and was not assigned to the monomeric dye. Assuming that all the dye molecules are in dimeric form and are bound to the polymer, we found $\mu_{0a} = 8.39$ D. For the ultraviolet transition, we took $\mu_{0b} = 9.41$ D, simply by assuming the ratio, μ_{0b}/μ_{0a}, to be equal to that in the case of the acridine orange-poly(S-carboxymethyl-L-cysteine) system.[22] Values of the optical parameters are listed in Table III.

The interaction potentials were found to be negative up to the fourth neighbors, and the interaction between the second neighbors ($l - k = 2$) was the strongest, as was expected. Figure 4 shows the calculated values of dipole strength and rotatory strength of the visible transition for the helical array of dimeric dyes.

Assuming the Gaussian band for each transition between the ground state and an exciton level[23], the molar ellipticity can be calculated by summing the contributions from N exciton levels, and is given by

$$[\theta]_E = \frac{48\pi^{3/2}N_A\nu}{hcN\Theta_E} \sum_{K=1}^{N} R_{EK} e^{-(\nu-\nu_{EK}/\Theta_E)^2} \tag{7}$$

where Θ_E is the half-width of the band which is assumed to be common to all the levels of the same electronic transition. We chose $\Theta_A = 1725$ cm^{-1} and $\Theta_B = 3400$ cm^{-1} as previously.[22] Calculated molar ellipticity was divided by 2, to convert the values from dimer to monomer and to compare with the observed ones. Calculated spectra are shown in Figure 5 and are compared with the observed spectrum for a solution of P/D 20 at pH 4.58. It is seen that the shape of the observed spectrum can be reproduced by calculated curves, except for the case of $N = 2$. The magnitude of each band is in the best agreement with that calculated for the array composed of 6 dimeric dye molecules ($N = 6$). Such a local aggregate of bound dye can be formed by the strong dispersion attractions between dimeric dye molecules, especially between the second neighbors which are situated in a position favorable for the stacking interaction.

TABLE III
Optical Parameters for the Dye-α-Helix Complex

Bound Species	E	$\frac{c}{\nu_{E0}}$ (nm)	μ_{oe} (D)	$\frac{\Theta_E}{c}$ (cm^{-1})
Dimer	A	458	8.39	1725
	B	261	9.41	3400
Monomer	A	492	5.93	1725
	B	261	6.65	3400

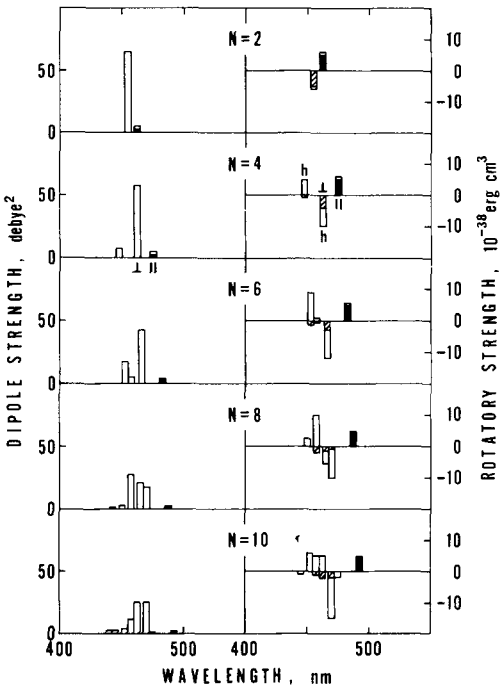

Fig. 4. Calculated dipole strengths and rotatory strengths of helices composed of different numbers of dimeric dye molecules. Left: D_{EK}/N. Solid bar: the first term of Eq. (1), i.e., $D_{EK\parallel}/3N$. Open bar: the second term of Eq. (1), i.e., $2D_{EK\perp}/3N$. Right: R_{EK}/N. Solid, hatched, and open bars represent the first ($\parallel$), second ($\perp$), and third (h) terms of Eq. (2) modified as follows:

$$R_{EK} = \frac{\pi\nu_{E0}}{3c} a\mu_{0e,\parallel}\mu_{0e,t}\left(\frac{D_{EK,\parallel}}{\mu^2_{0e,\parallel}} - \frac{2D_{EK,\perp}}{\mu^2_{0e,\perp}}\right) + \frac{1}{3}R^{\parallel}_{EK}.$$

Nonconservative Contribution

The above calculation of circular dichroism was based on the zeroth order perturbation, and only conservative circular dichroism was treated. In the previous observations on the acridine orange-β-form poly(S-carboxymethyl-L-cysteine) system, the nonconservative contribution of circular dichroism was found to be rather large:[15,22] i.e., the molar ellipticities of circular dichroic bands belonging to an electronic transition do not sum to zero. In the present system, i.e., the acridine orange-α-helical poly(L-glutamic acid) system, the observed circular dichroism is seen to be much less nonconservative, and, consequently, the first-order perturbation treatment was not included. The reason for this small nonconservative contribution may be explained as follows.

The helical array of N chromophores is assumed to have only two elec-

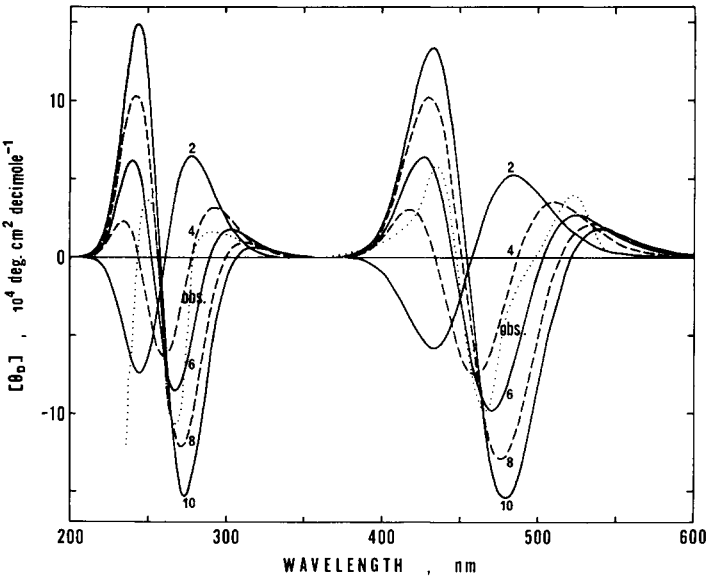

Fig. 5. Calculated circular dichroism for the acridine orange-α-helical-poly(L-glutamic acid) complex. Figures represent N. Dotted curve is the observed circular dichroism for the system of P/D 20, $[D] = 6.94 \times 10^{-5}\ M$ at pH 4.58.

trically allowed transitions, $0 - A$ and $0 - B$, whose electric dipoles are parallel to each other. This assumption would be justified for the discussion of circular dichroism of the visible transition, $0 - A$. Then the total rotatory strength for the transition, $0 - A$, is given by[23,24]

$$\sum_{K=1}^{N} R_{AK}^{(1)} = \frac{2\pi}{hc} \frac{\nu_{A0}\nu_{B0}}{\nu_{B0}^2 - \nu_{A0}^2}$$

$$\times \left\{ -a(\mu_{0a,t}\mu_{0b,\parallel} + \mu_{0a,\parallel}\mu_{0b,t}) \sum_{k=1}^{N} {\sum_{l\neq k}^{N}}' V_{k0a,l0b} \left[1 - \cos\frac{2\pi}{P}(l-k) \right] \right.$$

$$\left. + b(\mu_{0a,r}\mu_{0b,r} + \mu_{0a,t}\mu_{0b,t}) \sum_{k=1}^{N} {\sum_{l\neq k}^{N}}' (l-k) V_{k0a,l0b} \sin\frac{2\pi}{P}(l-k) \right\} \quad (8)$$

where $V_{k0a,l0b}$ is the interaction between electric dipoles for the transitions $0 - a$ in the kth and $0 - b$ in the lth chromophores, and the subscript r for μ_{0e} represents the radial component of the dipole moment. As was noted earlier in the calculation of conservative circular dichroism for our superhelix model, the interaction potentials were negative up to the fourth neighbors, and the interaction between the second neighbors ($l - k = 2$) was the strongest. The first and the third neighbor interactions were less than 1/3 and 1/6 of the largest, respectively. The relative magnitudes of the interaction potential between dipoles of different transitions are equal to those between dipoles of the same transitions, since these dipoles are both directed in the same direction. Accordingly, the first term of Eq. (8) is positive for our model. The second term of Eq. (8) is negative but its

magnitude would be less than that of the first term. Thus partial cancellation occurs and the contribution of nonconservative circular dichroism is small. This was actually confirmed by numerical calculation on the present model. On the other hand, in the dye-β-form complex, for which $P = 2$, the second term of Eq. (8) vanishes and no compensation occurs. Thus the first term of Eq. (8) yields nonconservative circular dichroism.[15,22]

Calculations for the Other Structures of the Complex

In the above-proposed model, the dye molecules were assumed to be bound to the polymer in the dimeric form, since the absorption spectra showed the presence of dimeric molecules almost exclusively. However, previous workers[3,19,25] have explained the induced optical activity in the present system, by postulating structures composed of monomeric dye molecules bound to the α-helix. We have, therefore, attempted to calculate circular dichroism of the complex, in which monomeric dye molecules are bound to the α-helix rather than dimeric molecules. The only alteration from the above model was in the values of electronic parameters used, which are given in Table III. Equation (6) was used without the factor 2, to estimate the value of μ_{0a}. Calculated values of interaction potentials, perturbation energy, and spectral strengths reduced to about a half of those for the dimeric case, and, consequently, visible circular dichroic bands shifted about 35 nm to the red and their magnitudes decreased to about $\frac{1}{3}$. The results do not agree with the observed ones, and the model based on the binding of monomeric dye molecules must be rejected.

Nevertheless, it is possible that some of the bound dye molecules are monomeric, since the weak shoulder of the absorption band around 500 nm is attributable to the monomeric dye. However, their amount is not so high that their contribution to circular dichroism might be overshadowed by the stronger dimer spectra, even if they are arranged to be optically active. Furthermore, it is rather difficult to include the interaction between bound monomer and bound dimer, since their mutual arrangement is indeterminable.

Apart from the problem of bound-dye species, which was confirmed to be dimeric, similar calculations of conservative circular dichroism were performed with some other models for the complex, by assigning appropriate values for geometric parameters. These models are summarized in Table II. The first two models are those in which the dimeric dye molecules anchor on third, (1-4), or fourth, (1-5), neighbors of carboxyl groups along the α-helix. The former can be formed only up to $N = 3$ and the latter to $N = 4$, owing to the steric hindrance. Numerical calculations actually yielded only two circular dichroic bands at each of the electronic transitions. Both models gave a negative band at longer wavelengths and a positive band at shorter wavelengths. Consequently, both of these models do not explain the observed result, which gives a spectrum of three circular dichroic bands at each transition.

In contrast to our right-handed superhelix model of bound dimeric dye molecules, Ballard et al.[3] deduced a left-handed superhelix of bound monomeric dye molecules. By means of the original Moffitt theory and the measurement of flow circular dichroism, they concluded that the longer axis of the dye molecular plane is almost parallel to the helical axis. They proposed a model of the complex in which each dye molecule anchors across three consecutive carboxyl groups, one at the middle and the other two at the third neighbors in both sides along the α-helix; as a result, a left-handed helix is formed. This model is similar to that given before as 1-4 in Table II, but the binding occurs at one and its third neighbors, 1-4-7. Later, this model was supported by Powers[26] from his measurement of electric birefringence on the same system but in dimethyl formamide. However, these workers[3,26] appear to have assumed that the superhelix of bound-dye molecules is formed by the binding at every seventh neighbor of the carboxyl groups. In this model, the nearest-neighbor interaction is the strongest but negative, and only a pair of conservative circular dichroism bands occurs. Actual calculation leads to a positive band at longer wavelengths and a negative band at shorter wavelengths. While the first term of Eq. (2), which was derived by Moffitt, leads to a negative band at longer wavelengths and a positive band at shorter wavelengths, the second term, which was missed by Moffitt and not taken into account by Ballard et al.,[3] has a much larger magnitude and makes a positive contribution to the circular dichroism at longer wavelengths and a negative contribution at shorter wavelengths. Thus the model proposed by Ballard et al.[3] does not conform with the observed circular dichroism, even if dimeric dye is substituted for monomeric dye. These considerations do not support the model proposed by Ballard et al.

References

1. Blout, E. R. & Stryer, L. (1959) *Proc. Nat. Acad. Sci.* **45,** 1591–1593.
2. Stryer, L. & Blout, E. R. (1961) *J. Amer. Chem. Soc.* **83,** 1411–1418.
3. Ballard, R. E., McCaffery, A. J. & Mason, S. F. (1966) *Biopolymers* **4,** 97–106.
4. Yamaoka, K. & Resnik, R. A. (1966) *J. Phys. Chem.* **70,** 4051–4066.
5. Sato, Y. & Hatano, M. (1973) *Bull. Chem. Soc. Jap.* **46,** 3339–3344.
6. Hatano, M., Yoneyama, M. & Sato, Y. (1973) *Biopolymers* **12,** 895–903.
7. Mason, S. F. (1963) *Nature* **199,** 139–141.
8. Tinoco, Jr., I. (1964) *J. Amer. Chem. Soc.* **86,** 297–298.
9. Holzwarth, G. & Doty, P. (1965) *J. Amer. Chem. Soc.* **87,** 218–228.
10. Myhr, B. C. & Foss, J. G. (1966) *Biopolymers* **4,** 949–952.
11. Eyring, E. J., Kraus, H. & Yang, J. T. (1968) *Biopolymers* **6,** 703–714.
12. Sato, Y., Yoneyama, M. & Hatano, M. (1972) *Bull. Chem. Soc. Jap.* **45,** 1941.
13. Sato, Y., Hatano, M. & Yoneyama, M. (1973) *Bull. Chem. Soc. Jap.* **46,** 1980–1983.
14. Zanker, V. (1952) *Z. Phys. Chem.* **199,** 225–258.
15. Ikeda, S. & Imae, T. (1971) *Biopolymers* **10,** 1743–1757.
16. Cassim, J. Y. & Yang, J. T. (1969) *Biochemistry* **8,** 1947–1951.
17. Imae, T. & Ikeda, S. (1975) *Biopolymers* **14,** 1213–1221.
18. Myer, Y. P. (1969) *Macromolecules* **2,** 624–628.
19. Tinoco, Jr., I., Woody, R. & Bradley, D. F. (1963) *J. Chem. Phys.* **38,** 1317–1325.

20. Zanker, V. (1954) *Z. Phys. Chem.* **2,** 52–78.
21. Zanker, V., Held, M. & Ramensee, H. (1959) *Z. Naturforsch.* **14B,** 789–801.
22. Ikeda, S. & Imae, T. (1973) *Polym. J.* **4,** 301–307.
23. Tinoco, Jr., I. (1968) *J. Chim. Phys.* **65,** 91–97.
24. Tinoco, Jr., I. (1962) *Advan. Chem. Phys.* **4,** 113–160.
25. Bradley, D. F., Woody, R. & Tinoco, Jr., I. (1963) *Biopolymers* **1,** 239–267.
26. Powers, Jr., J. C. (1967) *J. Amer. Chem. Soc.* **89,** 1780–1785.

Received December 1, 1975
Accepted April 9, 1976